

Leonid M. Lobanov, Nikolaj A. Pashchin, Igor P. Kondratenko, Yuriy M. Sidorenko, Pawel R. Ustimenko

# Electrodynamic Treatment of Structural Elements Made of Aluminium and Magnesium Alloys

**Abstract:** The article discusses the electrodynamic treatment (EDT) of thin-walled welded structures and EDT equipment, presents results of mathematical modelling concerning the effect of EDT on stresses in welded sheets made of aluminium alloy AMg6 as well as discusses the effect of EDT on the plastic strain mechanism. In addition, the article presents tests results concerning the effect of EDT during the welding of ship structures made of AMg6 plates and discusses the role of EDT in bulge formation. In addition, the article discusses the application of EDT during the repair welding of aero-engine nacelles made of magnesium alloy ML10 and the effect of EDT on openings in an airplane wing stinger in relation to its service life.

**Keywords:** electrodynamic treatment, aluminium alloys, magnesium alloys, welded joints, internal stresses, mathematical modelling, electroplastic effect, fabrication of aviation structures, shipbuilding

**DOI:** [10.17729/ebis.2021.2/2](https://doi.org/10.17729/ebis.2021.2/2)

## Introduction

High technical expectations concerning welded aviation, spacecraft and ship structures necessitate the development of their post-weld treatment being alternative to heat processing and characterised by the minimum consumption of energy. Prospective methods are based on the effect of electric pulsed current (EPC) and pulsed electromagnetic field (PEF) on the mechanical properties of metals, alloys and welded joints [1].

The effect of EPC and PEF takes place during a new technological process known as electrodynamic treatment (EDT) and aimed at the adjustment of stresses and strains of thin-walled welded structures made of light alloys. The effectiveness of EDT is determined by the interaction of two components, i.e. an electro-impulse component present during the flow of EPC (having density  $j \geq 1.0 \text{ kA/mm}^2$ ) through a product in the treatment zone and a dynamic component, adjusted by means of the amplitude-frequency characteristic of the

Leonid M. Lobanov, Academician of the National Academy of Sciences of Ukraine; dr hab. inż. Nikolaj A. Pashchin – E. O. Paton Electric Welding Institute, the National Academy of Sciences of Ukraine; Igor P. Kondratenko – Institute of Electrodynamics of the National Academy of Sciences of Ukraine, corresponding member of the National Academy of Sciences of Ukraine; dr hab. inż. Yuriy M. Sidorenko, inż. Pawel R. Ustimenko – National Technical University of Ukraine, Igor Sikorsky Kiev Polytechnic Institute

wave of stresses (initiated by electrodynamic forces). The interaction of the aforesaid wave of stresses with internal welding stresses combined with the simultaneous flow of EPC (where  $j \geq 1 \text{ kA/mm}^2$ ) results in the relaxation of the latter. The above-named relaxation is based on the electron-dislocation interaction known as the electroplastic effect (EPE) [1–3]. The use of EDT results in the formation of areas characterised by scattered metal structure, the evolution of which is triggered by EPE.

The study aims to identify the effect of EDT on stresses, strains and structural evolution as well as on the service life of welded joints made of aluminium and magnesium alloys used in the aviation and ship-building industries.

## Electrodynamic effect and EDT equipment

Based on the analysis of EPC power supply units it was ascertained that, as regards EDT, the most favourable solution should involve the use of capacitor systems, characterised by numerous advantages, including the possibility of accumulating a controlled level of energy and the adjustment of electric charge duration. A control element triggering electrodynamic effects is a flat induction coil (IC), being a part of the EDT discharge circuit.

A machine enabling the performance of the electrodynamic treatment of a welded joint 4 (see the schematic diagram presented in Figure 1) is composed of capacitive energy accumulator (CEA), power switch (K), flat coil (1), shield made of non-ferromagnetic material (2) and an electrode (3). Elements 1–3 make up an electrode device (ED). The electrode device (ED) is placed in the axis of the weld of a welded joint, fixed to mounting plate (5) by means a fixing load (q). After the capacitive energy accumulator (CEA) has been fully charged and with the power switch (K) being in the off-position, electric pulsed current flows through circuit elements 1–3 to 4. The flow of electric pulsed current through the induction coil triggers the

pulsed electromagnetic field in the coil and initiates eddy currents in the disc. The interaction of induced currents (I) with the pulsed electromagnetic field (PEF) (triggering eddy currents) generates electromagnetic force (P) in the induction coil (IC). The above-named electromagnetic force is responsible for pushing the disc away from the coil. With the electrode device (ED) fixed rigidly, at the moment when the electrode comes into contact with the weld surface, force P initiates the active (impact) load of the welded joint synchronised in time with the flow of electric pulsed current having density  $j \geq 1.0 \text{ kA/mm}^2$ . This, in turn, as a result of the electroplastic effect (EPE) leads to the local (i.e. in the area of the interaction of elements 3 and 4) relaxation of tensile internal welding stresses.

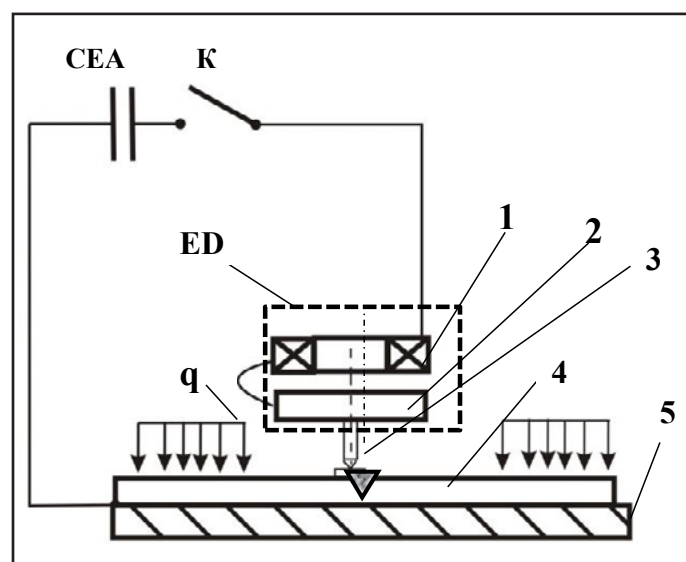


Fig. 1. Schematic diagram presenting the electrodynamic treatment (EDT) of welded joints: CEA – capacitive energy accumulator, K – power switch, q – fixing load, ED – electrode device, 1 – coil, 2 – disc, 3 – electrode, 4 – specimen and 5 – mounting plate

Taking into consideration the specific nature of welded aircraft, rocket and ship structures, including the considerable length of welded joints and their various arrangements in space, it is necessary to ensure the mobile positioning of equipment generating the electrodynamic effect. The specific nature of welded joints entails specific requirements in terms of EDT equipment:

- equipment for electrodynamic treatment should consist of separate components including the source of electric pulsed current (SEPC) and the electrode device (ED) as well as means of communication between the source of electric pulsed current (SEPC) and the electrode device (ED);
- ergonomic characteristic of the electrode device (ED) and the method of its communication with the source of electric pulsed current (SEPC) should ensure the easy operation of the EDT machine both in the manual mode and when the machine constitutes an element of an automated welding complex.

Presently available sources of electric pulsed current are provided with one or two channels (see Figure 2). A characteristic feature of the one-channel SEPC (Fig. 2, a) is the direct flow of electric pulsed current of the main circuit through a material subjected to treatment (see the schematic diagram in Figure 1). In turn, a characteristic feature of the two-channel SEPC is the separate flow of current through circuits providing electro-impulse and dynamic components of the electrodynamic effect.

The advantages of the one-channel source of electric pulsed current include the simplicity of design, relatively light weight (up to 20 kg) and small dimensions ( $450 \times 450 \times 250$  mm) as well as mobility and easy operation. In turn, the

disadvantages of the one-channel SEPC include the stepped adjustment of frequency characteristics of electrodynamic effect. The advantage of the two-channel SEPC (Fig. 2b) is the equipment-based adjustment of electrodynamic effect components. The disadvantages of the two-channel SEPC are relatively heavy weight (up to 120 kg) and significant dimensions ( $1500 \times 450 \times 450$  mm).

The performance of electrodynamic treatment using one-channel sources of electric pulsed current required the development of special electrode devices (Fig. 3) ensuring the electric contact between the source of electric pulsed current and a material being processes as well as providing the active loading of the processed material on one channel. The direction of electric pulsed current flow through the circuits of the electrode device from the source of electric pulsed current to a material being process is presented (using arrows) in Figure 3a. The working element of the electrode device (ED) is an electrode (1) mounted in a housing (2). The work surface of the electrode is in contact with the metal subjected to treatment. Along with the electrode (1), the housing (2), fixed rigidly with the disc (3), constitutes a part of the impact mechanism which can move in the vertical direction. The disc (3) is connected to the induction coil (4). Above the connection terminals there is a casing (5), which is also used for

the positioning of the electrode device (ED) during electrodynamic treatment. The electrode device is connected to the source of electric pulsed current (SEPC) using terminals 6 and 7 located at the top of the housing (2). Terminal 6 enables the flow of electric pulsed current (EPC) through the electrode, whereas terminal 7 enables the flow of electric pulsed current through the induction coil.



Fig. 2. Sources of electric pulsed current (SEPC) in electrodynamic treatment (EDT) processes: a) one-channel SEPC and b) two-channel SEPC



The design of the electric device used in the two-channel SEPC is similar to that presented in Figure 3, yet electric pulsed current (ECP) flows separately through the electrode (1) and the induction coil (4).

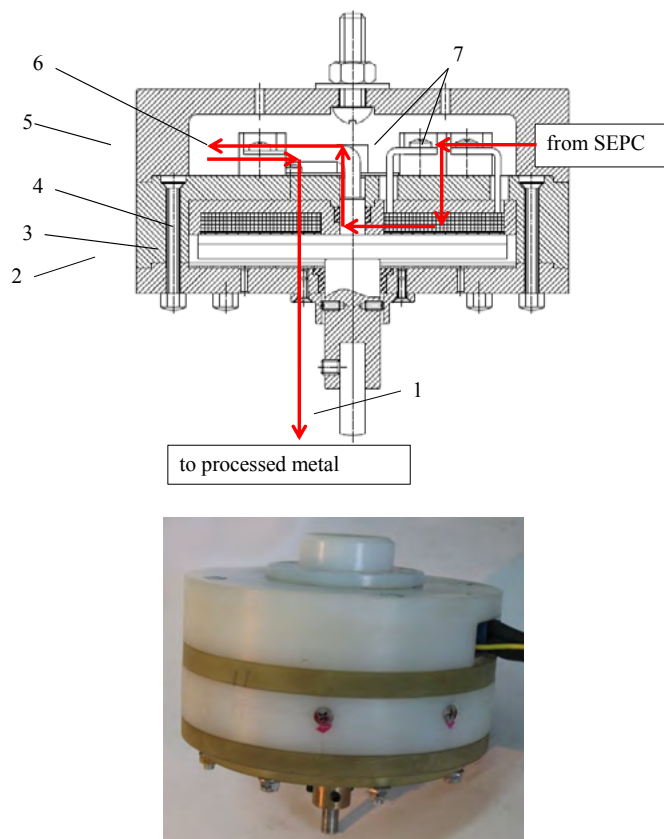


Fig. 3. Electrode device (ED) used in electrodynamic treatment (EDT): a) schematic diagram of the ED design, where 1 – electrode, 2 – housing, 3 – shield, 4 – coil, 5 – casing, 6 and 7 – terminals; b) main view of the electrode device (ED)

Figure 4 presents oscillograms of electromagnetic force (dynamic pressure) (P) and electric pulsed current (ECP) - I flowing through a sheet made of aluminium AMg6 having thickness  $\delta = 4.0$  mm (charging voltage  $U_{ch} = 500$  V, capacity of the capacitive energy accumulator (CEA)  $C = 6600$   $\mu$ F) – in accordance with the one-channel system. The characteristic feature of the one-channel system is invariably longer time of electric pulsed current (I) affecting the area of treatment than the time of force (P) effect. In the two-channel system, the independent change of I and P duration is controlled by the equipment, enabling the adjustment of various relations of

amplitude-frequency characteristics of the current effect and of the dynamic effect on the metal subjected to treatment.

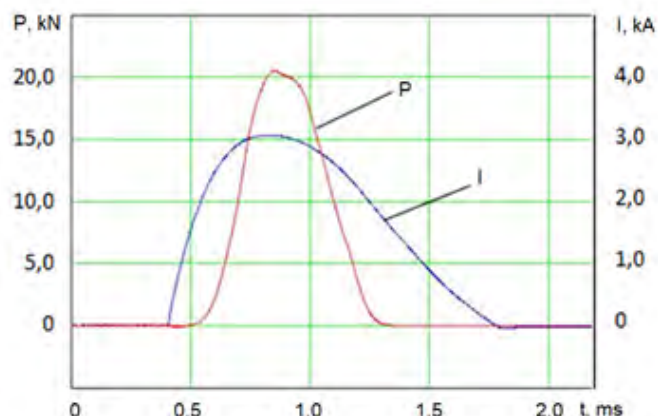


Fig. 4. Oscillograms of dynamic pressure (P) and pulsed current (I) flowing through the metal subjected to treatment; charging voltage  $U_{ch} = 500$  V, capacity  $C = 5140$   $\mu$ F and inductance  $L = 5.0$   $\mu$ H; one-channel discharge circuit

To ensure the positioning of the electrode device (ED) in relation to the processed surface of long welded joints it was necessary to develop a dedicated manual tool (Fig. 5).

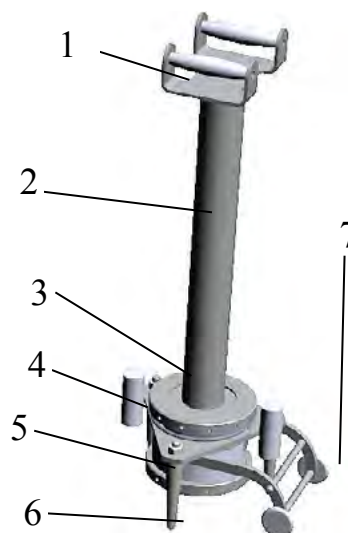


Fig. 5. Manual tool for electrodynamic treatment: 1 – fixed holder, 2 – base, 3 – mechanism fixing the electrode device (ED), 4 – light, 5 – electrode device (ED), 6 – support, 7 – cart

The structural elements of the tool include the base (2) with a fixed holder (1) and the mounting plate of the electrode device (ED) (3). The holder is used by the operator to move the tool. The plate is provided with the lighting of the EDT area (4), the electrode device (ED) (5)

and two support (6), which, along with the electrode device provide the three-point support of the tool on the processed metal surface. The tool is provided with a transport cart (7) used for moving and setting the electrode device (ED) along a welded joint. Based on data [4], it can be stated that electrodynamic treatment (EDT) accompanied by the simultaneous heating of an area subjected to processing is more effective as regards the control of stresses in metallic materials than EDT performed at room temperature. The aforesaid conclusion specifies initial EDT application conditions during welding processes, providing a number of advantages in comparison with the treatment of the welded joint after its cooling:

- increasing the efficiency of the welding process (by 50–70%) through the reduction of time of the welded joint treatment resulting from the combination of welding process time and electrodynamic treatment (EDT) time;
- reduction of energy consumption used to heat the welded joint before EDT by using heat generated during the welding thermal cycle;
- wide range of temperature of simultaneous heating, determined by the distance ( $L$ ) between the welding power source (2) and the electrode device (3) over the cooling fragment of the welded joint (Fig. 6), enabling the use of a wide range of metallic materials for the heating process;

- simplicity of design and possibility of automation;
- increasing the efficiency of electrodynamic treatment through the additional refinement of the structure of the welded joint metal as a result of electrodynamic effect combined with elevated temperature.

## Mathematical modelling of electrodynamic treatment (EDT)

The optimisation of EDT based on experimental results is a laborious task making it necessary to take into account many EDT regime parameters, types of welded joints and mechanical properties of processed metals and alloys.

To optimise the model of the EDT regime it was necessary to develop a mathematic model of non-stationary electrophysical [5] and dynamic [6] processes determining the mechanism of the electrodynamic effect. The model is used for selecting EDT characteristics aimed to control the internal stresses of alloy AMg6.

Electrophysical processes occurring during electrodynamic treatment were described on the basis of the reduction of Maxwell equations to integral equations concerning current density and electrodynamic forces present in the contact area between the electrode (3) and the specimen (4) (see Fig. 1). Figure 7 presents the distribution of lines of the same electric pulsed current (EPC) density –  $j$  across the thickness

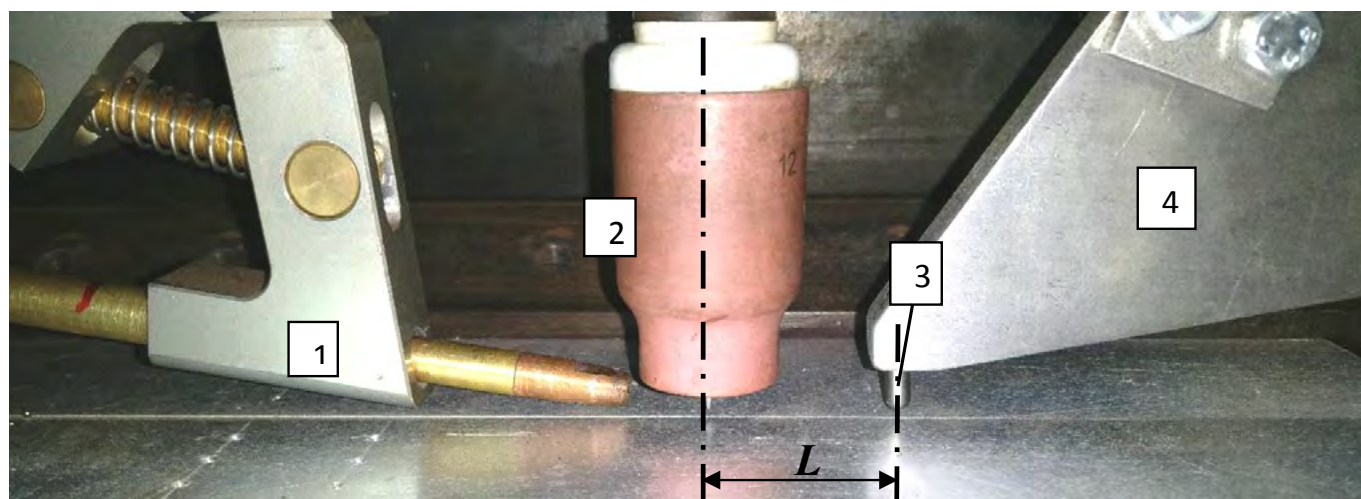


Fig. 6. Electrodynamic treatment (EDT) equipment used during welding: 1 – Bowden cable for filler metal wire feeding, 2 – TIG welding torch, 3 – electrode for EDT, 4 – dynamic load device 3,  $L$  – distance between 2 and 3

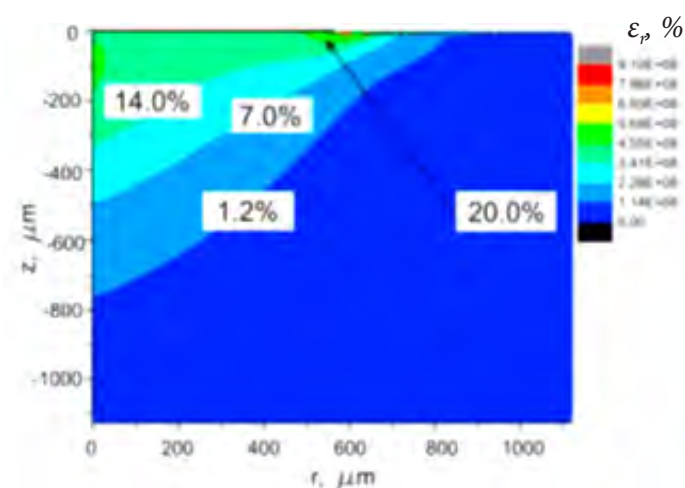
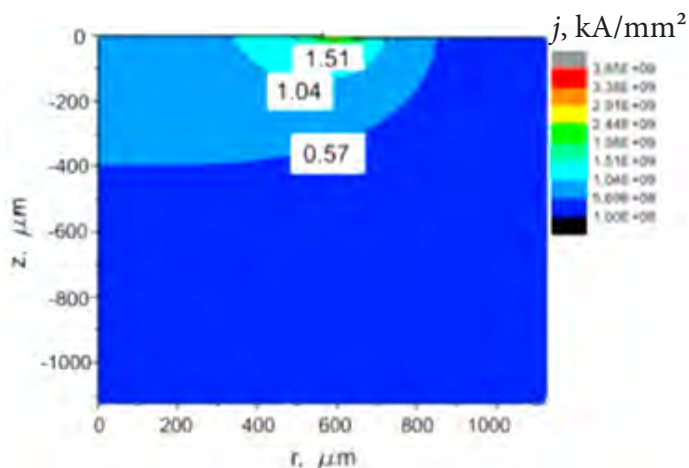


Fig. 7. Distribution of lines representing the same density of electric pulsed current (EPC) –  $j$  across the thickness the sheet made of alloy AMg6 (where  $L = 5 \mu\text{H}$ ,  $C = 5140 \mu\text{F}$ ,  $U_{ch} = 500 \text{ V}$  and  $t = 0.71 \text{ ms}$ ), corresponding to the maximum value of electric pulsed current (EPC) in the circuit

Fig. 8. Distribution of lines representing the same values of radial plastic strains  $\epsilon_r$  across the thickness the sheet made of alloy AMg6 (where  $L = 5 \mu\text{H}$ ,  $C = 5140 \mu\text{F}$ ,  $U_{ch} = 500 \text{ V}$  and  $t = 0.71 \text{ ms}$ ), corresponding to the maximum value of electric pulsed current (EPC) in the circuit

of the sheet made of alloy AMg6 (inductance of the electrode device (ED)  $L = 5 \mu\text{H}$ ,  $C = 5140 \mu\text{F}$ ,  $U_{ch} = 500 \text{ V}$  at  $t = 0.71 \text{ ms}$ ) corresponding to the maximum value of electric pulsed current in the discharge circuit. It can be noticed that the above-presented mode ensures the obtainment of values of current density  $j \geq 1 \text{ kA/mm}^2$ , initiating the electroplastic effect in alloy AMg6 subjected to treatment. The results of the electroplastic effect are confirmed by data shown in Figure 8, presenting distributions of lines

representing the same values of radial plastic strains  $\epsilon_r$  resulting from the tension across the thickness the sheet made of alloy AMg6 and exerted in the EDT regime analogous to that presented in Figure 7. The presented distribution of  $\epsilon_r$  is caused by the effect of electrodynamic forces generated when electric pulsed current (EPC) flows through the contact area between the electrode and the metal. Electrodynamic forces are responsible for the electroplastic strain of alloy AMg6 in the treatment area.

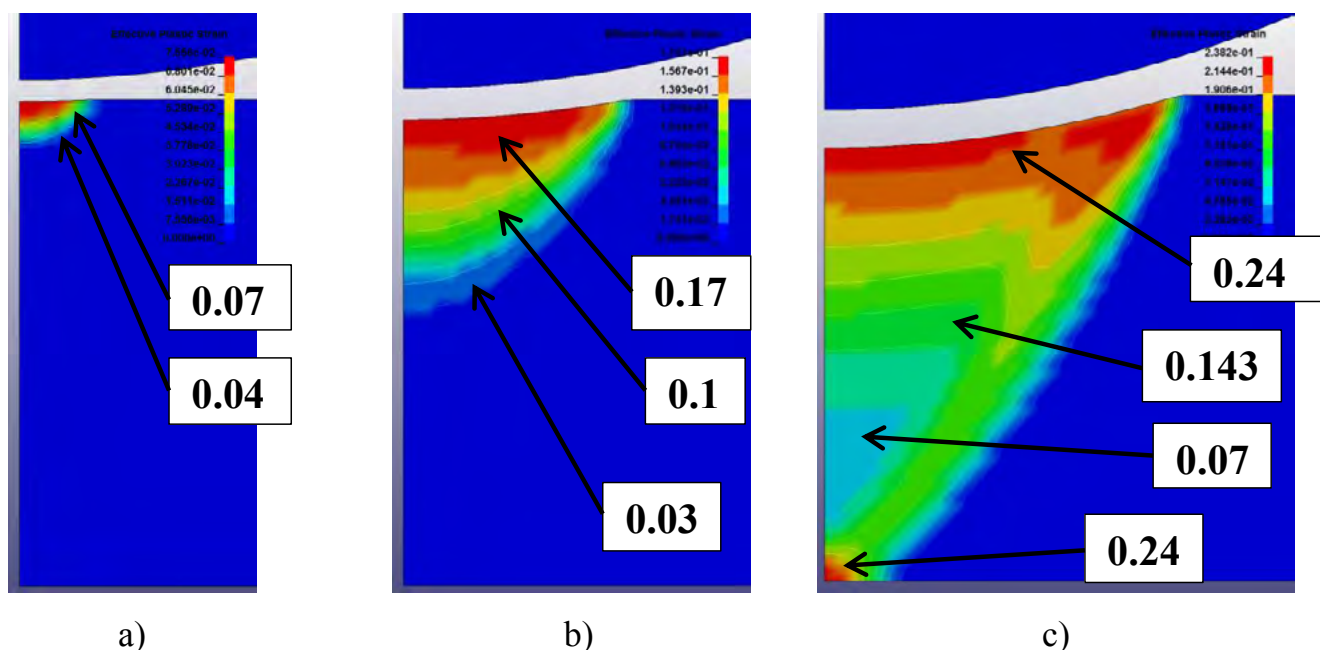


Fig. 9. Distribution of effective plastic strains  $\epsilon$  in the cross-section of the sheet made of alloy AMg6; (thickness  $\delta = 4 \text{ mm}$ ,  $L = 5 \mu\text{H}$ ,  $C = 5140 \mu\text{F}$  and  $U_{ch} = 200\text{-}800 \text{ V}$ : a)  $U_{ch} = 200 \text{ V}$ ; b)  $U_{ch} = 500 \text{ V}$ ; c)  $U_{ch} = 800 \text{ V}$



The interaction of EDT-triggered strains with plastic compressive internal (residual) strains decreases the state of stresses and strains in welded structures.

The influence of the dynamic component of the electrodynamic effect was determined on the basis of the plastic flow theory based on the Prandtl-Reiss equations. Figure 9 presents the distribution of effective plastic strains  $\epsilon$  in the cross-section of a non-loaded sheet made of alloy AMg6 (thickness  $\delta = 4$  mm, single ECP in the EDT regime,  $L = 5 \mu\text{H}$ ,  $C = 5140 \mu\text{F}$  and  $U_{ch} = 200\text{--}800$  V). It can be noticed that in relation to  $U_{ch} = 200$  V, the zone of plastic strain, restricted within the range  $\epsilon = 0.04 \div 0.07$ , is located just near the sheet surface (Fig. 9a).

An increase in  $U_{ch}$  up to 500 V is accompanied by the expansion of the plastic strain restricted within the range of  $\epsilon = 0.03 \div 0.17$  nearly to the central zone of the sheet cross-section (Fig. 9b). An increase in  $U_{ch}$  up to 800 V (Fig. 9c) initiates the propagation of the plastic strain restricted within the range of  $\epsilon = 0.07 \div 0.24$  across the entire cross-section of the sheet. In the above-named case, as opposed to the data presented in Figures 9a and 9b, the strain wave is reflected against the opposite surface of the sheet, which confirms the equality of the value of  $\epsilon_{ff}^p = 0.24$  on both sides of the specimen, and a decrease in the value in the centre of the specimen.

The data presented in Figure 9b are confirmed by the distribution of the radial component of internal stresses  $\sigma_r$  after single ECP in

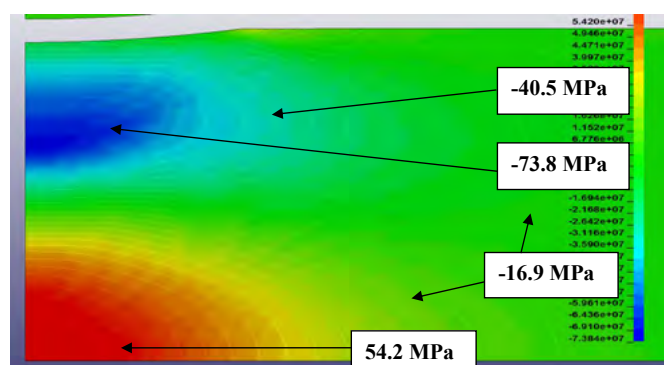


Fig. 10. Distribution of the radial component of internal stresses  $\sigma_r$  after single EPC in relation to  $U_{ch} = 500$  V

relation to  $U_{ch} = 500$  V (see Figure 10). It can be seen that the propagation of  $\epsilon$ , determined by the dynamic effect, is responsible (in and at a certain distance from the treatment area) for the generation of internal compressive stresses amounting to  $\sigma_r = -73.8$  MPa and  $-40.5$  MPa respectively. The superposition of  $\sigma_r$  compression with tensile internal welding stresses may significantly reduce the peak values of stresses in the welded joint.

In general, the analysis of the data presented in Figures 7–10 justifies the conclusion that electrodynamic and dynamic effect considered separately within the mathematical modelling of the EDT process significantly affect the state of stresses and strains of the non-loaded sheet made of alloy AMg6. The aforesaid statement is confirmed by experimental tests.

The modelling of the electrodynamic effect involved the assessment of the EDT effect on the stresses of the non-loaded sheet (Fig. 7–10) and the identification of stresses in the sheet in relation to EDT during welding. The state of stresses in a 2 mm thick sheet subjected to initial tension to value  $\sigma_0 x$  at various stages of the weld cooling process was determined in relation to the value of yield point  $\sigma_{0.2}$  and the coefficient of elasticity ( $E$ ) of alloy AMg6 at various temperatures. Component  $\sigma_0 x$  corresponds to the longitudinal component (along the weld line) of internal welding stresses at various stages of the weld cooling process. The values of  $\sigma_0 x$ ,  $\sigma_{0.2}$  and  $E$ , adopted as initial data for calculations based on method [6] in relation to various conditions are presented in Table 1. The adopted EDT regime was the same as that adopted for calculations, the results of which are presented in Figures 7–10.

Initially, the modelling involved electrodynamic treatment (EDT) performed at room temperature (Table 1, line 1) as well as in the weld areas where  $T = 150^\circ\text{C}$  and  $T = 300^\circ\text{C}$ . Calculations were concerned with values of stresses in the cross-section of the sheet in the areas of the probable failure of the weld, i.e. in

Table 1. Mechanical characteristics of the sheet made of alloy AMg6, subjected to initial tension at various temperatures

No.	Calculation conditions	T, °C	$\sigma_{0x}$ , MPa	$R_{0,2}$ , MPa	E, GPa
1.	EDT of metal without heating	20	150	150	71
2.	EDT metal behind the heated zone	150	120	120	65
3.	EDT of metal in the heated zone	300	50	50	55

the weld axis and along the fusion line (5 mm away from the weld axis). The distributions of the values of components of normal internal stresses  $\sigma_x$ ,  $\sigma_y$  and  $\sigma_z$  across the thickness of the sheet made of alloy AMg6 during EDT and welding heating are presented in Figure 11.

When analysing the data presented in Figure 11 it was possible to notice that the results of the EDT simulation at  $T = 150^\circ\text{C}$  (line 2 of Table 1) confirmed the positive effect of the thermoelastic heating of the contact effect area on the effectiveness of the treatment of alloy AMg6. The above-presented conclusion was based on the results of a comparison of the values of components  $\sigma_x$  (d),  $\sigma_y$  (e),  $\sigma_z$  (f) of the stresses present in the sheet subjected to EDT at  $T = 150^\circ\text{C}$  (line 2 of Table 1) with the values of components

$\sigma_x$  (a),  $\sigma_y$  (b),  $\sigma_z$  (c) of the stresses present in the sheet subjected to EDT at  $T = 20^\circ\text{C}$  (line 1). The analysis revealed that in relation to  $T = 150^\circ\text{C}$ , the values of components  $\sigma_x$ ,  $\sigma_y$  and  $\sigma_z$  of compressive stresses were higher than those at  $T = 20^\circ\text{C}$ . A further increase of  $T$  to  $300^\circ\text{C}$ , defined by the data provided in line 3, negatively affected values  $\sigma_x$  (g),  $\sigma_y$  (h) and  $\sigma_z$  (i) in comparison with previous calculation results. The obtained

results revealed that electrodynamic treatment combined with simultaneous heating was more effective than EDT performed at room temperature. The aforementioned observation provides the basis for the development of EDT technologies in relation to welding processes and constitutes the objective of future research.

## Effect of EDT on the evolution of structure, stresses, precision and the service life of welded joints made of alloy AMg6

Tests concerning the EDT-triggered structural evolution of structural materials made it possible to identify the electrodynamic effect on the mechanism responsible for the generation of plastic strains in metals and alloys. The features

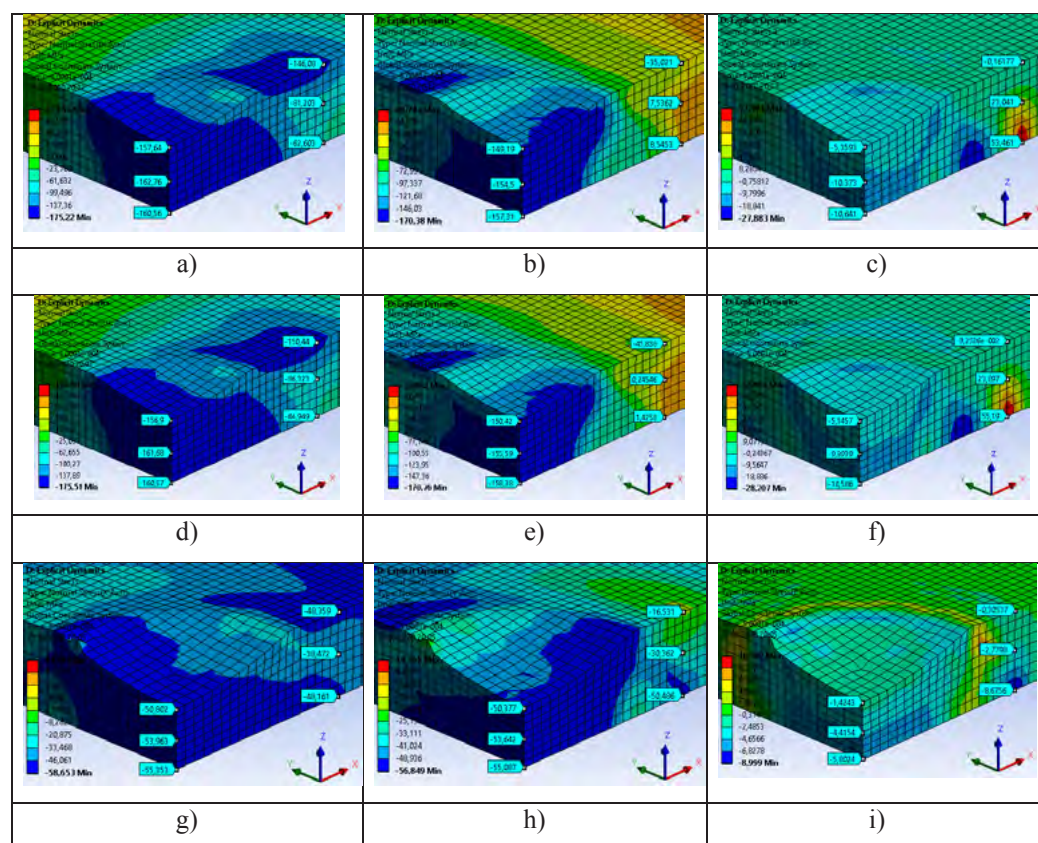


Fig. 11. Distribution of values of (MPa) components of normal internal stresses  $\sigma_x$  (a,d,g),  $\sigma_y$  (b,e,h),  $\sigma_z$  (c,f,i) across the thickness of the sheet made of alloy AMg6 in relation to EDT and modelled heating: a) c) – line 1 from Table 1; d) f) – line 2 and g) i) – line 3



of the structure and the relief of fractographs were examined using raster and scanning electron microscopy.

The investigation involved tests of the EDT effect on the nature of the cracking of alloy AMg6. The test involved the one-sided EPC treatment of 4 mm-thick flat specimens (150 mm × 30 mm) using charging voltage  $U_{ch} = 500$  V and  $C = 6600$   $\mu$ F. The results of the comparison of the microgeometry of cracks in specimens in the initial state (Fig. 12a) and after EDT (Fig. 12b) revealed that the structure of the fractures was predominantly fibrous, with detachment combs created by the mechanism of mixed cracking. Figure 12b (zone A) reveals that the fracture on the side subjected to EDT was characterised by the more developed fibrous structure if compared with the initial state (Fig. 12a). The depth of fibre propagation was 3.0 mm deep (in the specimen), which indicated that the electrodynamic is of volumetric nature. The more detailed examination of the fracture after EDT (zone B in Fig. 12b) revealed the presence of groups of flat slide lines, the orientation of which overlapped with the processed surface of the specimen. In the above-presented case, the slide had traces of the rotational mechanism, indicating the intense flow of plastic material affected by electrodynamic effect.

An increase in the cohesion of the processed areas of the polycrystalline structure led to work hardening, which was confirmed

by hardness (HV) measurement results. The hardness tests were performed using an M-400 machine (Leco) under a load of 0.1 N. The hardness values of the untreated material (Fig. 12a, zone B) amounted to 824 MPa. The maximum values, i.e. HV = 1290–1310 MPa, were observed near the processed surface (Fig. 12b, zone A), where the flat slide was accompanied by the rotational slide. As a result, the hardness of alloy AMg6 after EDT increased by 35–40% in comparison with the alloy not subjected to EDT. At the same time, the treated structure was characterised by grain refinement, increasing the resistance of the metal to post-weld cold cracking.

The initial subtle structure of alloy AMg6 as well as its evolution triggered by the dynamic and electrodynamic effect were examined using the thin-foil method. The dynamic effect was obtained by excluding the flow of electric pulsed current (EPC) through the metal subjected to the treatment. The electrodynamic treatment (EDT) involved specimens having dimensions 150 mm × 30 mm × 4 mm; charging voltage was  $U_{ch} = 350$  V, whereas the capacity of capacitive energy accumulator (CEA) was  $C = 6600$   $\mu$ F.

The test results (Fig. 13) revealed that the grains of the unprocessed metal were characterised by the substructure (Fig. 13a), the dimensions of which  $d_c$  was restricted within the range of approximately 1.8  $\mu$ m to 5  $\mu$ m and which was characterised by the uniform distribution of the density of the dislocation structure between volume  $\rho_{vol.}$  and grain boundary  $\rho_{gr.}$ . The value of  $\rho_{vol.}$  amounted to  $6 \times 10^9$   $cm^{-2}$ , whereas  $\rho_{gr.} \sim 8 \times 10^9$   $cm^{-2}$ , which led to the lack of the gradient of density of dislocations  $\Delta \rho_{vol.}$  within the volume of grains.

The metal after the dynamic treatment (Fig. 13b) was characterised by both a dispersive structure ( $d_c \sim 1.1$   $\mu$ m) and a structure characterised by significant dimensions ( $d_c \sim 3.2$   $\mu$ m), without the formation of clearly visible sub-boundaries. It was possible to observe an increase in the density of dislocations along

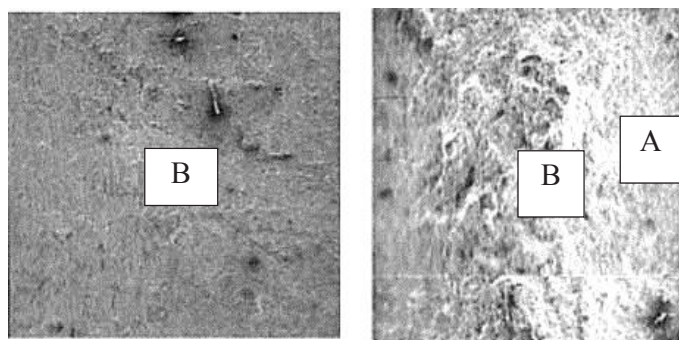


Fig. 12. Fractographs of fractures of alloy AMg6 obtained in relation to specimen fractures, where zone A – processed area near the metal surface, zone B – central part of the fracture: a) without EDT; b) after EDT (mag. 33x)

grain boundaries  $\rho_{gr}$ , and gradient  $\Delta\rho_{vol}$ . between the internal volume of grains  $\rho_{vol} \sim 6 \times 10^8 - 4 \cdot 10^9 \text{ cm}^{-2}$  and  $\rho_{gr} \sim 2 \times 10^{11} \text{ cm}^{-2}$ .

The metal after the electrodynamic treatment contained substructures (Fig. 13c) with clearly visible boundaries  $d_c = 0.8 - 2.5 \text{ }\mu\text{m}$ . The metal subjected to EDT was characterised by a decrease in the density of dislocations  $\rho_{gr}$  in comparison with the metal subjected to the dynamic effect. In addition, the dislocations were distributed uniformly within the entire volume of the metal, (without significant gradients along grain boundaries  $\Delta\rho_{gr}$ ) between the internal volume of grains  $\rho_{vol} \sim 2 - 3 \times 10^{10} \text{ cm}^{-2}$  and along grain boundaries  $\rho_{gr} \sim 6 - 8 \cdot 10^{10} \text{ cm}^{-2}$ .

The formation of the structure confirmed the proposed concept (based on the theory of electron-dislocation effect [1]) concerning the contribution of electric pulsed current (ECP) to the relaxation of internal stresses.

The assessment of the EDT effect on internal welding stresses involved the performance of butt joints made of alloy AMg6 ( $400 \text{ mm} \times 300 \text{ mm} \times 4 \text{ mm}$ ) with the central weld made using automatic TIG welding (arc voltage  $U_d = 18 \text{ V}$ , welding current  $I = 250 \text{ A}$  and welding rate  $V_{sp} = 3.1 \text{ mm/s}$ ). The two-sided treatment of the welded sheets was performed using a series of electric pulsed current in the EDT mode (charge voltage  $U_{ch} = 550 \text{ V}$ , capacity  $C = 6600 \text{ }\mu\text{F}$ ). The distance between the zones subjected to the electrodynamic effect did not exceed  $5 \text{ mm}$ .

Internal stresses were measured using the electronic speckle interferometry technique [7]. The distributions of the longitudinal component (along the weld line) of internal stresses  $\sigma_x$  in the central cross-section of the sheet before and after EDT are presented in Figure 14. As can be seen, the maximum output values of  $\sigma_x$  in the weld axis (WA) and in the partially melted zone (PMZ) amounted to  $120 \text{ MPa}$  and  $90 \text{ MPa}$  respectively (curve 1). After EDT, stresses in WA and PMZ,  $10 \text{ mm}$  away from

the weld axis (curve 2) changed from tensile to compressive and their value ( $\sigma_x$ ) amounted to  $-75 \text{ MPa}$  and  $-90 \text{ MPa}$ , respectively. The zone of the assumed crack in welded joints of alloy AMg6, triggered by cyclic loads (where the effect of internal welding stresses is one of the dominant factors responsible for the rupture), overlapped with the partially melted zone. Based on the foregoing it could be stated that the maximum efficiency of the electrodynamic treatment is obtained through the sequential treatment of the weld axis and the partially melted zone near the fusion line.

The research also involved the tests of the EDT effect on the fatigue strength of the welded joints made of alloy AMg6 having thickness  $\delta = 2 \text{ mm}$ . The welded specimens were made using the automatic argon-shielded TIG welding process ( $U_d = 20 \text{ V}$ ,  $I = 170 \text{ A}$  and  $V_{sp} = 5.5 \text{ mm/s}$ ). The two-sided electrodynamic treatment (EDT) along the  $90 \text{ mm}$ -long weld line was performed using  $U_{ch} = 430 \text{ V}$  and  $C = 5580 \text{ }\mu\text{F}$ . The distance between the zones subjected to the electrodynamic effect amounted to  $5 \text{ mm}$ . The fatigue bending tests of the welded joints were performed using a symmetric cycle with the amplitude of oscillation of cycle stresses restricted within the range of  $2 \cdot \sigma_a = 80 - 160 \text{ MPa}$ . The tests involved taking into account the number of cycles preceding the failure ( $N$ ). Figure 15 presents the results of the fatigue tests in relation to the coordinates of  $2 \cdot \sigma_a - N$  of the specimens in the as-received state and after EDT. It can be noticed that, after the treatment, the values of  $N$  of the specimens within the tested range of  $2 \cdot \sigma_a$  increased as many as three times. In such a case, both the specimens in the as-received state and those subjected to EDT ruptured along the fusion line.

The above-presented results revealed that EDT positively affected the fatigue strength of the welded joints made of alloy AMg6, primarily through the reduction of internal welding stresses.

The fractographic analysis of the microrelief

of the specimens in the as-received state and after EDT (ruptured as a result of a cyclic load where  $\sigma_a = 160$  MPa (Fig. 16)) revealed that the metal subjected to the electrodynamic treatment was characterised by the dispersion of structural elements (3-fold refinement of dimension of facets (Fig. 16b)) in comparison with the initial state preceding EDT (Fig. 16a).

The foregoing confirmed the positive effect of electrodynamic treatment on the evolution of the structure of the metal demonstrated by its increased fatigue crack resistance.

The level of internal stresses determines the warping parameters of welded structures. The research also involved the performance of tests aimed to determine the effect of electrodynamic treatment (EDT) on local distortions ("bulges") formed during the welding of ship structures composed of sheets. The tests involved 4 mm thick sheets made of alloy AMg6 (Fig. 17), to which stiffeners were welded using the TIG method and the following parameters:  $U_d = 20$  V,  $I = 180$  A and  $V_{sp} = 1,4$  mm/s. The making of the specimens was followed by the measuring of the value of sagging  $f$  in the middle of the specimen (Fig. 17a). Afterwards, the convex surface of the specimen was treated with a series of impulses using a step of 10 mm as well as  $U_{ch} = 500$  V and  $C = 6600$   $\mu$ F. Figure 17b presents changes in the shape of the sheet before and after EDT. It can be noticed that, as a result of the electrodynamic effect, sagging  $f$  decreased from 8 mm to 1.6 mm, which is an acceptable value as regards welded hull structures made of aluminium alloys.

## Prospective applications of EDT in the aviation and shipbuilding industries

Electrodynamic treatment (EDT) enables the extension of the service life and the reduction of internal stresses and strains in various types of welded structures. The use of EDT in the production and repair of ships made of alloy AMg6 made it possible to increase operating

characteristics of products. The EDT-based straightening of the plating and elements of load-bearing structures improved the hydrodynamic properties of ship hulls. The straightening of bulges decreased local sags in the area of welded joints from 10 mm to 1.5 mm, whereas the reduction of the curvature of beams in the bottom reinforcement zone from 8 mm to 0.5 mm improved the adhesion of the bottom plating. At the same time, the electrodynamic treatment of repair welded joints of the hull and the framework of the structure decreased internal stresses from 150 MPa to 40 MPa, enabling the 2-6-fold extension of the service life of ships (depending on operating conditions).

A structural element of the AN-74 aircraft is an aero-engine nacelle (AEN), tasked with the attachment of the D-36 engine to the wing. The aero-engine nacelle is a large-sized cast hollow structure made of high-temperature creep resisting magnesium alloy ML10 (M/110). The structure is composed of cylindrical external and internal shells connected by means of stiffening ribs. Coolant flows in internal chambers (Fig. 18a). Typical defects of aero-engine nacelles (AEN), eliminated using repair welding, are fatigue cracks, affecting the integrity of the internal and external shell as well as damage to the front face of the external shell in the reinforcement zone under the flange of the cooling pipeline. In the above-named case, the maximum values of the longitudinal component (along the weld) of tensile internal welding stresses  $\sigma_x$  in repair welds not subjected to heat treatment reach 120 MPa, which is close to value  $\sigma_{0.2}$  for alloy ML10. In some cases, the elimination of stresses performed using heat treatment exceeds the cost of repair welding. An alternative to heat treatment is electrodynamic treatment (EDT), the use of which makes it possible to significantly reduce costs of post-weld heat treatment. Unlike heat treatment, which entirely eliminates internal stresses, in terms of EDT, stress  $\sigma_x$  in the weld axis and in the partially melted zone



(“near-weld zone”) changes in the cross-section of the welded joint from tensile to compressive (Fig. 18b). Figure 18b shows that the value of  $\sigma_x$  before and after EDT reached 120 MPa (curve 1) and -40 MPa in the weld axis (WA) (curve 2) respectively and was similar to the value in the partially melted zone (PMZ) (curve 3) [8]. Unlike heat treatment, eliminating internal stresses within the entire volume of the metal of the aero-engine nacelle (AEN), the effect of electrodynamic treatment is limited to its zone, which can be perceived as a disadvantage. However, taking into consideration the low cost of EDT, the method is likely to find its niche in aircraft repair technologies.

The competitiveness of airliners and cargo aircraft depends primarily on their optimum weight characteristics. The pursuit of service life restricted within the range of 60 thousand to 80 thousand flight hours combined with the necessary minimisation of the structure weight require the implementation of new methods enabling the extension of the fatigue service life of aircraft structure elements.

To reduce the amount of aircraft fuel (which is not used or disposed of), stringers of lower wing panels are provided with single openings or systems of openings enabling the flow of fuel (Fig. 19). The operation of aircraft and ground tests revealed that such openings are centres of fatigue cracks and may lead to the premature failure of the wing structure.

An increase in the fatigue strength of the lower panels of the aircraft wing in the fuel flow opening zone involves the use of various technological methods, most of which are based on local deep plastic strains (LDPS) within the area of the opening. The above-named methods include the barrier cold work and forcing through (applied both jointly and separately), involving the local deformation of the material and the generation of internal compressive stresses in the zone of increased concentration [9]. In spite of their high efficiency, the LDPS-based methods also have disadvantages, including the

relatively large size of LDPS equipment and the fact that the technological cycle of the treatment of one opening lasts up to 10 minutes.

The use of EDT to obtain LDPS (based on the electrodynamic forcing of an appropriately shaped punch in the opening area) seems promising. In comparison with the traditional LDPS methods, electrodynamic treatment enables the mobility of stamp positioning, which, in turn, makes it possible to subject openings to treatment in various positions in space. In addition, the time of treatment is significantly shorter than that of drawing.

The schematic LDPS diagrams were analysed using the EDT method (LDPS EDT). The analysis was performed in order to create the area of compressive stresses within the opening area and trigger the plastic strain on its surface (Fig. 20). The schematic diagram of a discharge circuit used in the LDPS-based EDT is presented in Figure 20a. A stringer (2) (resting on a rigid base) is located between a stamp (1) and a die (3). The stamp is rigidly connected with a disc (6) made of a non-ferromagnetic material, which, in turn, is the base of a flat induction coil (5). After starting a capacitor (C) discharge cycle using a contactor (K), repulsive electrodynamic force is generated between the induction coil and the disc. The vector of the force is directed along the normal to the stringer plane. The effect of electrodynamic force on the stamp and the die initiates their insertion in the material to be processed, thus generating LDPS within the opening area. The three proposed LDPS EDT variants include an EDT-forcing through process (Fig. 20b), a joint EDT-forcing through-cold work process (Fig. 20c) and an EDT-cold work process (Fig. 20d). The difference between the EDT-forcing through process and the traditional forcing through process consists in the replacement of a mandrel drawn through the opening with the cylindrical stamp (1) and the die (3), the work surfaces of which have the form of truncated cones. The electrodynamic effect of the stamp (1) and of the die

(3) on the metal provides the LSPS-based treatment of the stringer (2) opening surface. In the above-presented case, the intensity of plastic strain can be adjusted by changing the level of accumulated energy and electric pulsed current.

The joint EDT–forcing through–cold work technology (Fig. 20c) is a variant of the EDT–forcing through process, where an appropriately-shaped stamp (1) and a matrix (3) (in addition to generating the LDPS of the opening) provide cold work of the metal on the stringer area behind the opening zone. In such a case, the conical parts of the tool (inserted in the processed element during the LDPS-based process) ensure the alignment of the stamp and of the die in relation to the edge of the opening. During the EDT–cold work process (Fig. 20d), the alignment of the stamp (1) and of the die (3) in relation to the stringer (2) opening is ensured by a cylindrical guiding sleeve (4). The tests involved stringers with openings (6) mm made of aluminium alloy D16. The opening areas of the stringers subjected to LDPS EDT (as presented in related diagrams – see Fig. 20) in the mode determined by accumulated energy  $C = 800$  J. The non-destructive method-based processing [10] was followed by the recording of internal compressive stresses  $\sigma_y$  in the zone of the presumed propagation of fatigue cracks; the maximum value of  $\sigma_y$  amounted to  $-120$  MPa.

The performance of the tests was accompanied by the ongoing recording of the number of cycles preceding the failure ( $N$ ) in relation to the off-zero cycle of tensile load  $\sigma_{\max} = 200\text{--}203$  MPa.

Diagrams of  $\sigma_{\max} = f(N)$  in relation to the LDPS EDT specimens are presented in Figure 21 a. It can be noticed that EDT–forcing through (column 2) and EDT–forcing through–clamping (3) increase (by 1.6 times) value  $N$  in relation to  $\sigma_{\max} \sim 200$  MPa, whereas EDT–clamping (4) – by 2.5 times. The LDPS EDT process is shown in Figure 21 b. The presented data obtained in the tests justify the conclusion that the proposed LDPS EDT variants

make it possible to increase the resistance of the opening. Taking into consideration the technological potential of the method, including the compactness, fast operation and the mobility of the tool, electrodynamic treatment seems promising in terms of its applications in the aviation industry.

## Summary

The observations made during the practical use of electrodynamic treatment (EDT) revealed that the aforesaid type of treatment could find applications in various welding engineering areas. Because of their simplicity (in comparison with those based on the two-channel power supply sources), EDT technologies based on one-channel power supply sources can be used to straighten thin-walled welded structures. In turn, technologies based on two-channel power supply sources can be more useful in the reduction of internal welding stresses. Promising is also the use of EDT combined with the thermal-strain welding cycles to ensure the deformation-free welding of critical structures.

## References

- [1] Baranov Yu.V., Troitsky O.A., Avramov Yu.S.: Physical fundamentals of electro-pulse and electroplastic treatment and new materials. MGIU, Moscow, 2001. p. 844
- [2] Lobanov L.M., Pashchin N.A., Loginov V.P., Smilenko V.N.: Change of the stress-strain state of welded joints of aluminium alloy AMg6 after electrodynamic treatment. The Paton Welding Journal, 2007, no. 6, pp. 7–14.
- [3] Lobanov L.M., Pashchin N.A., Cherkashin A.V., Mikhoduj O.L., Kondratenko I.P.: Efficiency of electrodynamic treatment of aluminium alloy AMg6 and its welded joints. The Paton Welding Journal, 2012, no. 1, pp. 2–6.
- [4] Stepanov G.V., Babutskiy A.I., Mameyev I.A. Nestatsionarnoye

- napryazhenno-deformirovannoye sostoyaniye v dlinnom sterzhne, vyzvannoye impul'sami elektricheskogo toka vysokoy plotnosti. Problemy prochnosti, 2004, no. 4, pp. 60–67.
- [5] Lobanov L.M., Kondratenko I.P., Zhyltsov A.V., Karlov O.M., Pashchyn M.O., Vasyuk V.V., Yashchuk V.A.: Electrophysical unsteady processes in the system to reduce residual stresses welds. Tekhnichna elektrodynamika. 2016, no. 6, pp. 10–19.
- [6] Lobanov L.M., Pashchyn M.O., Mykhodui O.L., Sydorenko Y.M.: Effect of the Indenting Electrode Impact on the Stress-Strain State of an AMg6 Alloy on Electrodynamic Treatment. Strength of Materials. 2017, vol. 49, no. 3, pp. 369–380.
- [7] Lobanov L.M., Pivtorak V.A., Savitsky V.V., Tkachuk G.I.: Method of determination of residual stresses in welded joints and elements of structures using electron speckle-interferometry. Avtomaticheskaya svarka. 2006, no. 1, pp. 10–13.
- [8] Lobanov L.M., Pashchin N.A., Mikhodui O.L., Khokhlova J.A.: Investigation of residual stresses in welded joints of heat-resistant magnesium alloy ML10 after electrodynamic treatment. Journal of Magnesium and Alloys, 2016, vol. 4, no. 2, pp. 77–82.
- [9] Grebenikov A.G., Krivov G.A., Vasilevskiy Ye.T.: Eksperimental'noye issledovaniye vliyaniya posledovatel'nogo primeneniya dornovaniya i bar'yernogo obzhatiya na ustalostnuyu dolgovechnost' stringerov v zone otverstiya dlya peretekaniya topliva. Otkrytyye informatsionnyye i kompp'yuternyye integrirovannyye tekhnologii: Sbornik. nauch. trudov Nats. Aerokosm. Un-ta im. N.Ye. Zhukovskogo «KHAИ». Vyp. 43. Charkov, 2009, pp. 54–64.
- [10] Gushcha O.I., Smilenko V.N., Kot V.N.: Kontrol' napryazheniy na osnove ispol'zovaniya podpoverkhnostnykh akusticheskikh voln. Tekhn. Diagnostika i nerazrushayushchiy kontrol'. 2009, no. 1, pp. 11–13.